



Growth of coronene on (100)- and (111)-surfaces of fcc-crystals



Tobias Huempfer, Falko Sojka, Roman Forker, Torsten Fritz*

Friedrich-Schiller-Universität Jena, Institut für Festkörperphysik, Helmholtzweg 5, 07743 Jena, Germany

ARTICLE INFO

Article history:

Received 9 March 2015

Accepted 24 April 2015

Available online 4 May 2015

Keywords:

Coronene

Potassium chloride

Silver

Copper

Nanographene monolayers

Polycyclic aromatic hydrocarbon (PAH)

ABSTRACT

The growth of coronene thin films is studied via low-energy electron diffraction (LEED) and scanning tunneling microscopy (STM) comparing metal substrates with different lattice constants, different surface symmetry, and also with surface passivation, namely Cu(111), Ag(111), Ag(100), and (100)-terminated KCl/Ag(100). In particular, we investigate the evolution of the coronene lattice parameters upon coverage- and temperature-variation. On the pristine metal surfaces we observe disordered phases at low coverage. Further deposition leads to hexagonal arrangement of the molecules. With increasing coverage the lattice constant decreases continuously, whereas on Cu(111) the molecular unit cell additionally rotates w.r.t. the substrate lattice. We also discuss the interaction mechanisms that are responsible for this behavior. Due to the continuous change in the lattice dimensions we observe many incommensurate structures that were stable during our measurements, however the close-packed structures we found were always commensurate. The use of a passivation layer leads to the formation of a bulk-like structure consisting of molecules adsorbed in an upright standing manner which is stable at low temperatures only.

© 2015 Elsevier B.V. All rights reserved.

1. Introduction

Polycyclic aromatic hydrocarbons (PAHs) with conjugated π -electron systems have recently attracted tremendous attention in various scientific communities. For instance, the formation of Cooper pairs in several $[n]$ acenes and also in coronene ($C_{24}H_{12}$, CAS registry number: 191-07-1) has been concluded from photoemission spectroscopy (PES) of the molecules in the gas phase [1]. In fact, following the discovery of superconducting phases of alkali-metal-intercalated picene [2] also K_x coronene samples (x = stoichiometric ratio) have been reported to become superconducting for a relative potassium content of $x = 2.5$ – 3.5 atoms per coronene [3]. These reports are based on measurements of the magnetic susceptibility χ of bulk samples showing characteristic drops at the critical temperatures T_c upon cooling at zero magnetic field. On the other hand, PES data of K_x coronene films with $x \approx 3$ showed no indication of emission from the Fermi level E_F , i.e., no electronic density of states was detectable at E_F [4]. In order to clarify the electronic ground state, band structure calculations, which are known to be rather sensitive to the crystal structures assumed, were performed [3,5]. While the bulk crystal structure of coronene has been determined quite precisely by means of X-ray diffraction (XRD) from powder samples [3] and from natural single crystals [6], thin films structures – investigated previously on $MoS_2(0001)$ [7,8], graphite(0001) [7–10], Ag(111) [10,11], Ag(110) [12], and Au(111) [13] – depend naturally on the substrate symmetry and lattice constants.

Here, we study the growth of coronene thin films by comparing metal substrates with different lattice constants, different surface symmetry, and also with surface passivation, namely Cu(111), Ag(111), Ag(100), and (100)-terminated KCl/Ag(100). We investigate the evolution of the coronene lattice parameters upon coverage- and temperature-variation by means of high precision low-energy electron diffraction (LEED) and scanning tunneling microscopy (STM), revealing several phase transitions from disordered or even moderately ordered to highly ordered structures. While coronene grows (mostly) in a flat-lying manner on the metal surfaces, the adsorption geometry on the KCl-film is upright with a molecular unit mesh comparable to the arrangement in the bulk, though slightly compressed. The comparison of our structural data to those of K_x coronene [14] can be regarded as a puzzle piece for a better understanding of the origin of the observed superconductivity [3], or possibly for the vanishing electronic density of states at E_F in thin films [4].

2. Experimental

All experiments were carried out in an ultra-high vacuum (UHV) chamber at a base pressure in the low 10^{-10} mbar range. During the preparation, deposition, and LEED experiments the sample is kept on a manipulator that can be cooled by cryogenic liquids and heated by a tungsten filament. From there the sample is transferred into the scanning tunneling microscope (STM) without interrupting the vacuum. The metal crystals were prepared by repeated sputtering with Ar^+ ions ($p = 2 \times 10^{-6}$ mbar, $E_{ion} = 700$ eV, $\vartheta = \pm 45^\circ$) for 30 min from two opposite directions and subsequent annealing ($T \approx 730$ K). Coronene was purchased from Sigma-Aldrich and purified via

* Corresponding author.

E-mail address: torsten.fritz@uni-jena.de (T. Fritz).

temperature gradient sublimation. KCl was cut from bulk single crystals and milled in a porcelain mortar. After transferring the obtained coronene and KCl powders to the UHV chamber they were thoroughly degassed for several hours before usage. Coronene and KCl were evaporated from quartz glass and boron nitride effusion cells, respectively. During the deposition of KCl the sample temperature was held at $T = 425$ K as suggested by Müller et al. [15] and Guo et al. [16], while KCl was evaporated at a source temperature of about 750 K. Due to the increased sample temperature the Ag(100) surface is homogeneously covered with KCl and only a minor fraction remains uncovered. The film quality was checked by room temperature STM measurements that are shown in the supplementary material Fig. S1. During the deposition of coronene ($T \approx 430$ K) onto the bare metal surfaces the sample was held at room temperature, whereas during the deposition on KCl/Ag(100) the sample was cooled with liquid nitrogen ($T \approx 80$ K). The surface coverages are estimated using the deposition time under the assumption of constant molecular flux and a coverage-independent sticking coefficient. We define one monolayer equivalent (MLE) as the amount of coronene necessary for a single layer of flat-lying molecules exhibiting the densest packing motif observed. Owing to the possible adsorption of molecules in the second layer before completion of the first, and considering the limited capabilities of LEED and STM for a quantitative determination of the surface coverage, the absolute uncertainties of the film thicknesses given in the following are estimated to be on the order of 0.1 MLE. However, the submonolayer films investigated exhibit pronounced structural changes for coverage increments well below 0.1 MLE (cf. Results and discussion section), hence their relative coverages are given with an apparent precision of two decimal places without claiming an absolute accuracy of 0.01 MLE.

Structural characterization was performed with a dual microchannel-plate LEED (MCP-LEED, OCI Vacuum Microengineering) in order to minimize the primary electron current. The inherent distortions and systematic errors of the recorded diffraction images were corrected using the recently introduced commercially available software *LEEDCal* [17,18]. Following this procedure, the reciprocal space dimensions were calibrated with well-known Si(111)-(7 × 7) and commensurate PTCDA/Ag(111) superstructures as reference samples [19,20], yielding highly precise results for the unit cell parameters and epitaxial relations. A high precision analysis of the LEED images measured was performed via *LEEDLab* by numerical fitting a simulated structure to the spots found [21]. All observable spots of one structure are simultaneously used leading to higher accuracy than usual (cf. Supplementary Material Fig. S2). The given uncertainties are the statistical errors of the fit results (confidence level 68%). The cubic lattice constants used for the evaluation of the LEED patterns are: $a_{\text{Cu}} = 3.6146$ Å and $a_{\text{Ag}} = 4.0853$ Å [22,23]. All LEED images shown are contrast-inverted, i.e., dark areas correspond to high intensity. STM is performed in a commercially available system (JT-STM/AFM with KolibriSensors [24], SPECS Surface Nano Analysis) at a temperature of 1.1 K providing stable measurement conditions and a significantly reduced lateral mobility of the molecules on the surfaces.

3. Results and discussion

3.1. Coronene on Ag(100)

We first deposited coronene on Ag(100) until a coverage of ca. 0.6 MLE is reached. The LEED pattern shown in Fig. 1(b) suggests that there is no long-range-ordered growth. This can be concluded from the rings that appear around every spot of the silver substrate. The diameter of those rings corresponds to the average distance between neighboring molecules, which we estimate as 15.8 Å. Here we take into account that, in essence, the molecules are coordinated almost hexagonally, which can be concluded from the associated STM image shown in Fig. 1(a) (note the six small red circles on the rings in Fig. 1(b), indicating the hexagonal coordination assumed for the determination of the molecular spacing).

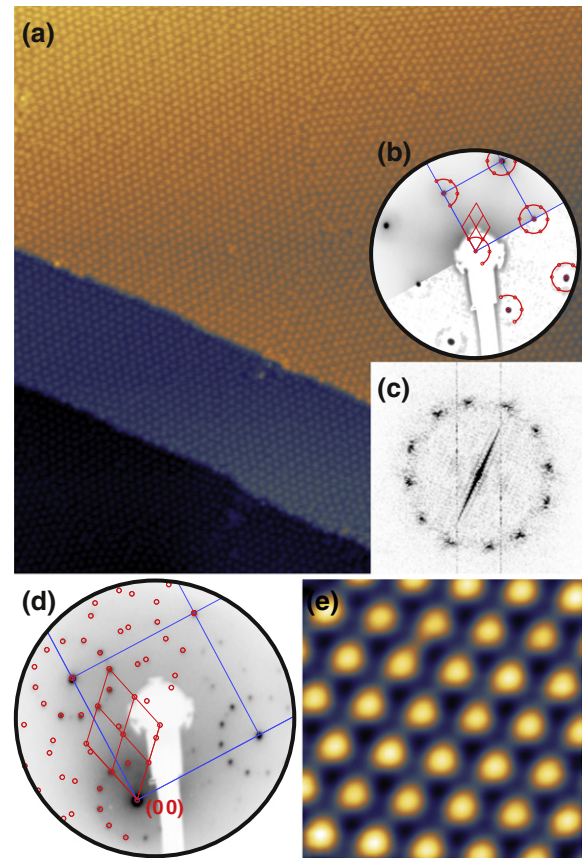


Fig. 1. Structural analysis of about 0.6 MLE (a)–(c) and 1 MLE (d)–(e) coronene on Ag(100). (a) STM image (100×100 nm², $V_t = 1.5$ V, $I_s = 50$ pA). (b) LEED pattern at 300 K, $E = 140.3$ eV (lower part: contrast enhanced for better visibility of the rings). (c) FFT of the STM image revealing preferential orientations of the two domains depicted (2.18×2.18 nm⁻²). (d) LEED at 300 K, $E = 56.5$ eV, tilted off-normal by 11° in order to image the (0 0)-spot and to access higher order reflexes simultaneously. (e) STM (6.3×6.3 nm², $V_t = 1.0$ V, $I_s = 60$ pA).

Interestingly, there are clearly two different rotational domains discernible on the upper terrace. At the first glance, this seems to be surprising regarding the structureless rings visible in the LEED pattern Fig. 1(b): disordered structures should not form domains. However, this apparent contradiction is easily lifted considering that the LEED pattern was obtained at room temperature, while the STM image was acquired at 1.1 K. Further insight is provided by comparing the fast Fourier transform (FFT) of the STM data (Fig. 1(c)) with the LEED pattern obtained again at room temperature but for a coverage of 1 MLE (Fig. 1(d)). From that it is apparent that the two domains appearing at low temperatures are already precursors for the final highly ordered high coverage structure characterized by mirror domains under angles of $\pm 14^\circ$ (see below), albeit still showing limited long-range order.

At a coverage of 1 MLE the LEED pattern in Fig. 1(d) shows defined spots that correspond to a highly ordered structure of the molecules with the following epitaxy matrix:

$$\begin{pmatrix} \vec{c}_1 \\ \vec{c}_2 \end{pmatrix} = \begin{pmatrix} 4.00 \pm 0.02 & 1.00 \pm 0.02 \\ -3.01 \pm 0.01 & 3.01 \pm 0.01 \end{pmatrix} \begin{pmatrix} \vec{a}_1 \\ \vec{a}_2 \end{pmatrix}. \quad (1)$$

Therefore, within the experimental errors a commensurate growth of the coronene adlayer on the Ag(100) surface is found. As opposed to coronene adlayers on hexagonal surfaces, e.g., on Ag(111) [9], the molecular arrangement on Ag(100) differs slightly from a perfect hexagonal unit cell due to the quadratic lattice of this silver surface. In detail, the first lattice vector $|\vec{c}_1| = (11.92 \pm 0.05)$ Å is smaller than the

Download English Version:

<https://daneshyari.com/en/article/5421842>

Download Persian Version:

<https://daneshyari.com/article/5421842>

[Daneshyari.com](https://daneshyari.com)